Tribology Letters (2019) 67:98
https://doi.org/10.1007/s11249-019-1200-9

ORIGINAL PAPER

Effect of Adding Tungsten Disulfide to a Copper Matrix on the Formation of Tribo-Film and on the Tribological Behavior of Copper/Tungsten Disulfide Composites

Lin Zhao[1] · Pingping Yao[1] · Taiming Gong[1] · Haibin Zhou[1] · Minwen Deng[1] · Zonghao Wang[1] · Zhongyi Zhang[1] · Yelong Xiao[1] · Fenghua Luo[1]

Received: 15 October 2018 / Accepted: 14 March 2019 / Published online: 1 August 2019

Abstract
The tribological behavior and formation of tribo-film of copper/tungsten disulfide (WS_2) composites featuring 0–30% WS_2 volume fractions, prepared using spark plasma sintering were investigated. Results indicated that WS_2 as addition into the copper matrix could effectively reduce the coefficient of friction (COF) of Cu/WS_2 composites. The lowest COF obtained was 0.16, while the wear rate was approximately 5×10^{-5} $mm^3{\cdot}N^{-1}{\cdot}m^{-1}$ for the Cu/WS_2 composite which contained 25vol% of WS_2 (here defined as Cu-25WS_2). X-ray photoelectron spectroscopy and transmission electron microscopy analyses indicated that an oxygen-rich tribo-film with a thickness of approximately 10 nm was formed on the wear track, while a thick layer which was rich in WS_2 and Cu_2S and with a thickness of approximately 50 nm was observed below the oxygen-rich tribo-film. The superior tribological properties could ascribed to the formation of these tribo-films.

Keywords Copper matrix composites · Tribological properties · Tungsten disulfide · Tribo-film · Wear mechanism

1 Introduction

Copper matrix self-lubricating composites containing lead, which exhibit a low coefficient of friction (COF) and high wear resistance are widely used as bearings, bushes, etc. Due to the technology developments and environmental, health and safety requirements, these composites should be gradually eliminated and substituted by high-performance lead-free materials [1–8]. Major efforts have been devoted to solving these concerns and meeting these expectations.

Layer-structured solid lubricants, such as graphite, MoS_2, hexagonal boron nitride (h-BN), copper/tungsten disulfide (WS_2) composites, etc., are some of the noteworthy substitute solid lubricants used because of their high stability and long service performance. Among them, metal sulfides, such as MoS_2 and WS_2, present a hexagonal lamellar structure, high melting points and chemical stability, and demonstrating good self-lubrication especially under high temperature in vacuum conditions. Due to the strong S-Mo-S and S-W-S covalent binding forces, the bonding strength between adjacent layers due to van der Waals forces is relatively small. Thus, interlamellar sliding can easily take place when these materials are subjected to shearing forces. Therefore, composites containing such substances will always exhibit lower COF and wear rates [9–14]. Additionally, both W and Mo belong to the sixth subgroup (VI B) of the periodic table and present similar chemical properties. However, compared to MoS_2, WS_2 presents a superior load resistance, higher temperature resistance, wider temperature service capability, longer lubrication life, lower COF, etc. [11, 15–17].

Several meaningful studies on Cu matrix composites consisting of MoS_2 and lubricating particles have been conducted to improve their tribological performance. Kovalchenko et al. [18] revealed that the lubricating effect was more pronounced when the concentration of solid lubricant was greater than 5 wt% for the Cu/MoS_2 and Cu/$MoSe_2$ composites. Cao et al. [19] found that the Cu/WS_2 composite containing 24 vol% WS_2 (Cu-24WS_2) presented a superior mechanical performance and lower wear rate compared to a Cu/graphite composite containing the same volume fraction

✉ Pingping Yao
yaopingpingxx@sohu.com

✉ Fenghua Luo
fenghualuo@csu.edu.cn

[1] State Key Laboratory of Powder Metallurgy, Central South University, Changsha 410083, China

of graphite (Cu-24G). Wang et al. [20] indicated that adding WS_2 as a lubricant substantially reduced the wear rate of the Cu matrix composites fabricated using spark plasma sintering (SPS). Moreover, the optimum WS_2 content that conferred the best friction properties to the composite was 20 wt%. Juszczyk et al. [21] studied the tribological properties of copper composites containing graphite, WS_2, MoS_2, and glassy carbon lubricating particles. The best tribological properties were achieved for the composites containing graphite and WS_2 particles. It could be concluded from these results that the layered structure of the solid lubricants could improve the tribological performance of the composites. To investigate the formation of tribo-films on the worn surface of self-lubricating composites, Xiao et al. [22] confirmed that a layer of lubricating film rich in MoS_2 formed on the worn surface while testing the tribological properties of the Cu/MoS_2 composites. Qian et al. [15] demonstrated that the contact resistance of the Cu/WS_2/G composites decreased but their wear rates increased. This could be caused by the adverse effects of the electrical current softening the materials at "a-spots" and damaging the tribo-film. However, currently, there has been very limited research concerning the formation of tribo-films of Cu/WS_2 composites. Moreover, the structure and composition of tribo-films have never been clearly characterized since testing them is difficult. Therefore, it would be significant to investigate the tribological behavior of Cu/WS_2 composites, and the effect of adding WS_2, on the formation of tribo-films, especially by analyzing the formation process of tribo-films and their influence on the tribological properties.

In this study, Cu/WS_2 composites containing 0, 5, 10, 15, 20, 25, and 30 vol% WS_2 were prepared using SPS. To investigate their tribological properties, friction and wear testing of the prepared composites was performed under a load of 10 N under atmospheric conditions. The microstructures and compositions of the tribo-films of the Cu/WS_2 composites were analyzed. Considering the small thickness and complex composition of the tribo-films, focused ion beam (FIB) and transmission electron microscopy (TEM) techniques were used to characterize the tribo-films in this study. The purpose of this study was to investigate the influence of the volume fraction of WS_2 on the tribological behavior of Cu/WS_2 composites, and to provide an accurate method for analyzing the structure and composition of the tribo-films formed on the worn surface.

2 Materials and Experimental Methods

2.1 Materials Preparation

As showed in Fig. 1a, b, commercially available WS_2 powder with an average size of 1.2 μm and Cu powder with an average size of 38.3 μm were used as raw materials. Since the tiny WS_2 particles aggregated together, a long ball milling process was used to uniformly mix the composite powders.

To avoid chemical reactions between the WS_2 and the Cu matrix, SPS was used in this work since it involved rapid heating and sintering. First, mixtures of certain ratios of Cu and WS_2 powders were combined using a planetary mill at a speed of 80 rpm for 24 h. A 6-mm-diameter brass milling ball was used, and the weight ratio of the brass ball to the mixture was approximately 3:1. Then, the homogeneously mixed powders were wrapped into a graphite die for SPS. Sintering was carried out at 750 °C under a pressure of 40 MPa for 15 min in a nitrogen atmosphere. Afterward, the specimens were cooled using water at a cooling rate of approximately 100°C/min. Thus, specimens 40 mm in diameter and 5 mm thick were prepared.

2.2 Friction and Wear Testing

A friction testing machine (MM-W1B; Lanzhou Institute of Chemical Physics, China) with a ball-on-block test configuration was used for the tribological property tests. A steel ball bearing (AISI52100, 0.95–1.05C, 0.20–0.40Mn, 0.15–0.35Si, 1.30–1.65Cr, $S \leq 0.020$, $P \leq 0.027$, $Mo \leq 0.10$, $Ni \leq 0.30$, $Cu \leq 0.25$, $Ni + Cu \leq 0.50$), which was 4 mm in

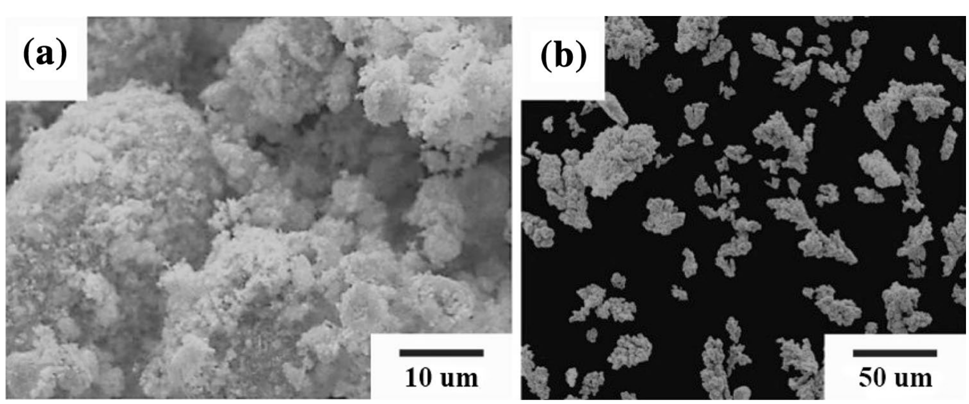

Fig. 1 SEM images of **a** WS_2 and **b** Cu powders

in diameter and had a hardness of 63–65 HRC was selected as the testing ball. The obtained samples were ground and polished using SiC grit paper until surface roughness (Ra) values of 1.2 µm were obtained. The specimens were subsequently cleaned using anhydrous alcohol. The tests were conducted at a constant normal load of 10 N, a fixed sliding distance of 5 mm, a reciprocating speed of 600 rpm (0.1 m/s) and a test time of 900 s. The average length (mm) and cross-sectional area (mm^2) of the wear tracks were obtained by a 3D surface profilometer, and then multiplied to obtain the wear volume. The wear rate ($mm^3 \cdot N^{-1} \cdot m^{-1}$) was evaluated utilizing the volume of wear tracks using Eq. (1):

$$\text{Wear rate} = V/(f \cdot L) \quad (1)$$

where V is the wear volume (mm^3), f is the friction force (N) and L is the friction distance (m). Three parallel tests were performed for each sample, for each definitive set of test conditions.

2.3 Microstructural Characterization

The porosity of the Cu/WS_2 composites was measured by Archimedes' method following GB/T 1423-1996 (State Standard of China). The compressive strength of the Cu/WS_2 composites was obtained through an electronic universal testing machine (Model 3369; Instron, USA) with a sample size of Φ8 mm × 10 mm. The microstructures, morphologies of the worn surfaces, phase constituents, and tribo-films of the Cu/WS_2 composites before and after testing were investigated using field-emission scanning electron microscopy (SEM; Nova NanoSEM230; FEI, USA) coupled with energy dispersive spectroscopy (EDS). The average roughness of the sample surfaces was characterized using white light interferometry (Contour GT-K; Bruker, Germany). The phase composition of the specimens was analyzed using X-ray diffraction (XRD; DX-2700B; Dandong Haoyuan Instruments, China) employing Cu-Ka radiation. The length and cross-sectional area of the wear tracks was measured by a 3D surface profilometer (Nano Map 500-LS; AEP Technology, USA). The depth distribution of the elements with respect to the worn surface of the Cu/WS_2 was analyzed by using X-ray photoelectron spectroscopy (XPS; Escalab 250Xi system; Thermo Fisher, UK). This device was equipped with an Al-Kα X-ray excitation source (1486 eV) and was operated in constant analyzer energy mode with a pass energy of 100 and 30 eV for survey and high-resolution spectra, respectively. Ar^+ ions with an energy of 3 keV were used for etching the worn surface in order to measure the distribution of elements in depth. The size of the etched area was 2×2 mm^2 and the etching rate was approximately 0.33 nm/s. We performed XPS measurements at accumulated etching times of 0, 100, 400, 700 and 1000 s, respectively. Furthermore, transmission electron microscopy (TEM; JEM-2100F; JEOL, Japan) was used to characterize the morphologies and compositions of the worn surfaces, especially those of the tribo-films with the working voltage of 200 kV. Samples for the TEM investigation were prepared by using FIB cutting technology with the cutting direction perpendicular to the sliding direction on the worn surface. To prevent the worn surface from being destroyed during the FIB cutting, a protective layer of Pt was first used to cover the worn surface of the wear tracks.

3 Results and Discussion

3.1 Microstructure of Cu/WS_2 Composites

Table 1 illustrates the compositions of the powders before and after SPS, as well as the porosity and compressive strength of the specimens. The porosity increased as the percentage of WS_2 increased, while the compressive strength decreases, which was consistent with the results reported in the literature [16, 17].

Figure 2a–d presents the optical metallographic images of the Cu/WS_2 composites containing 0, 10, 20, and 30 vol% WS_2, respectively. The gray phases in Fig. 2 represent the Cu matrix, while the shallow black phases represent WS_2 particles. Moreover, the deep black phases in Fig. 2e represent pores. As observed in Fig. 2a–d, the number of WS_2 particles and pores continuously increased as the amount of added WS_2 increased. In addition, the distribution of the WS_2 particles appeared to be more homogeneous as the content of WS_2 of the composites increased, since more and more network microstructures between Cu and WS_2 were generated. As shown in Fig. 1, the WS_2 particles were much smaller than those of the Cu. The agglomeration of WS_2 particles could still be easily observed for the Cu/WS_2 composites, as shown in Fig. 2b–d. Moreover, the connections between the Cu matrix phases decreased due to the increased isolation caused by the increased volume fraction of the WS_2 particles. However, the interface area between

Table 1 Composition and mechanical properties of Cu/WS_2 composites

Sample	Cu (vol%)	WS_2 (vol%)	Porosity (%)	Compressive strength (MPa)
Cu	100	0	0.4	586.5
$Cu-5WS_2$	95	5	2.6	540.7
$Cu-10WS_2$	90	10	3.8	526.9
$Cu-15WS_2$	85	15	4.9	512.1
$Cu-20WS_2$	80	20	5.3	497.3
$Cu-25WS_2$	75	25	5.9	486.4
$Cu-30WS_2$	70	30	6.5	470.1

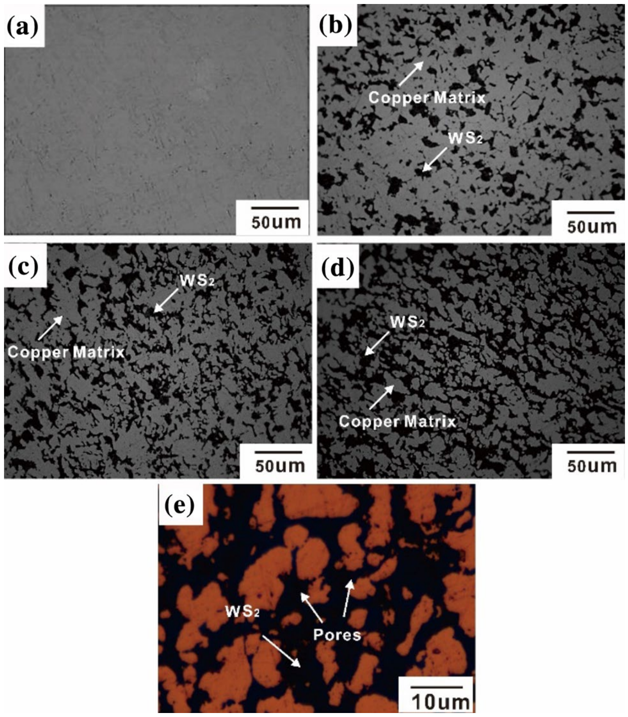

Fig. 2 Optical metallographic images of Cu/WS_2 composites containing **a** 0, **b** 10, **c** 20, and **d** 30 vol% WS_2, and **e** highly magnified image of (**d**)

the WS_2 particles and the Cu matrix increased as the volume fraction of WS_2 increased, which enabled more chemical reactions between the WS_2 particles and the Cu matrix to occur.

Figure 3 shows the XRD patterns of the WS_2 powder and Cu/WS_2 composites. It should be noted that WS_2 peaks were observed for all the Cu-WS_2 composites, and obvious Cu_2S peaks could be detected for both Cu-25WS_2 and Cu-30WS_2. However, for the Cu/WS_2 composites containing 5–20 vol%WS_2, very few/no Cu_2S peaks were detected. This could be ascribed to the reaction between the WS_2 particles and the Cu matrix. The equation of the corresponding chemical reaction could be described as follows [23, 24]:

$$4Cu + WS_2 = 2Cu_2S + W \quad (2)$$

As illustrated in Fig. 4, the free energy (ΔG) of Eq. (2) was obtained by linearly fitting the following equation:

$$\Delta G = -0.1152T + 120 \quad (3)$$

When the free energy (ΔG) was zero, the theoretical temperature of the reaction between WS_2 and Cu would be 1042 K (744 °C). Given that the sintering temperature was higher than the theoretical reaction temperature, WS_2 particles could theoretically react with the Cu matrix. Therefore, this confirms that the SPS technique could effectively prevent the reaction between Cu and WS_2.

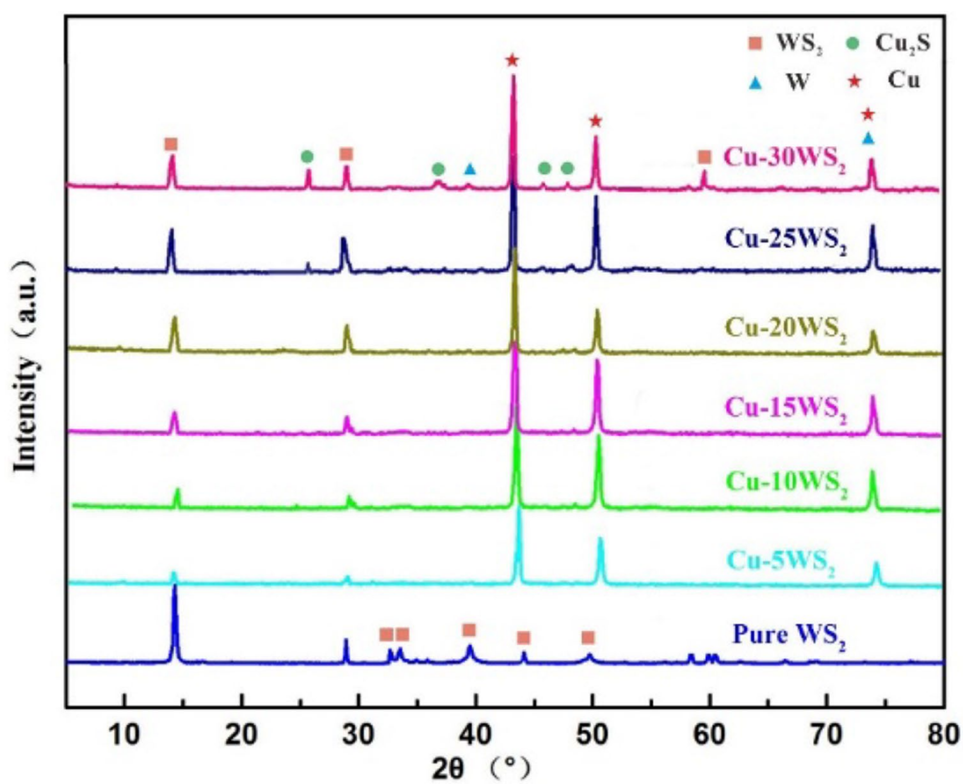

Fig. 3 XRD patterns of WS_2 powder and Cu/WS_2 composites

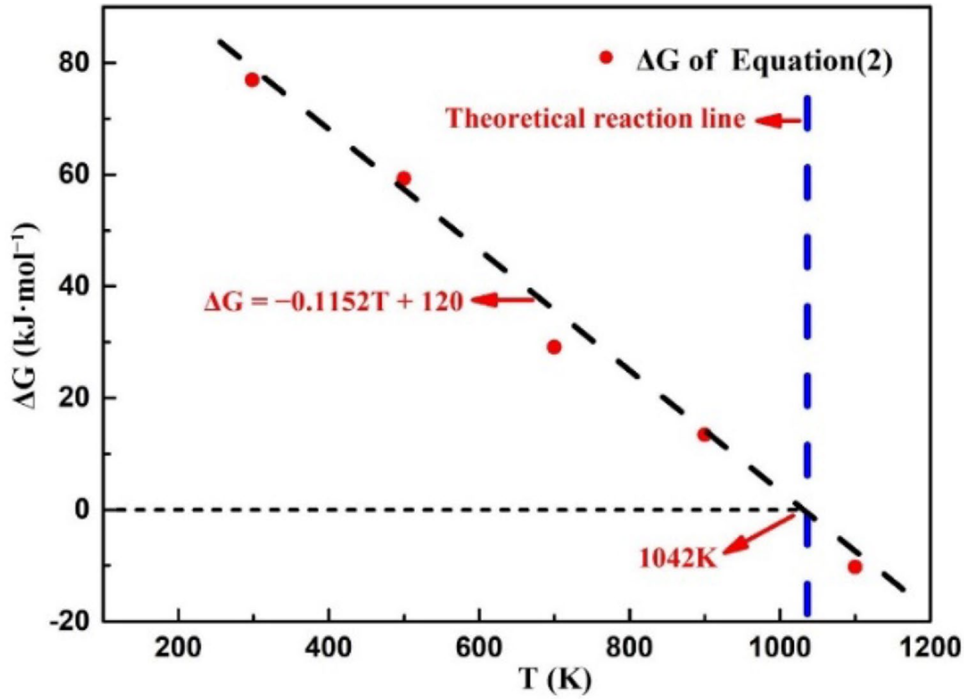

Fig. 4 ΔG for Eq. (2) at different temperatures (kJ mol^{-1}) [23, 24]

3.2 Friction Coefficient and Wear Rate

Figure 5a shows the typical COF dependence on the testing time for the Cu/WS_2 composites. Relatively significant fluctuations in COF were observed when pure Cu was tested. However, as more WS_2 particles were incorporated into the Cu matrix, the COF curves became fundamentally different. Compared to the COF of pure Cu, those of the Cu/WS_2 composites obviously decreased and became stable during testing. This could be ascribed to the different wear mechanisms of the composites. The strong adhesive forces between the worn surfaces and work hardening could be the main factor influencing the tribological behavior of pure Cu. However, the WS_2 particles, as a solid lubricant, could prevent the direct contact between the two sliding surfaces during testing. The great reduction in COF of the Cu/WS_2 composites, compared to that of pure Cu, was probably due to the smeared WS_2 layer between the two surfaces in contact. The variations in the calculated average COF for the Cu/WS_2 composites containing different volume fractions of WS_2 is shown in Fig. 5b. As the volume fraction of WS_2 increased, the average COF gradually decreased, from 0.43 for pure

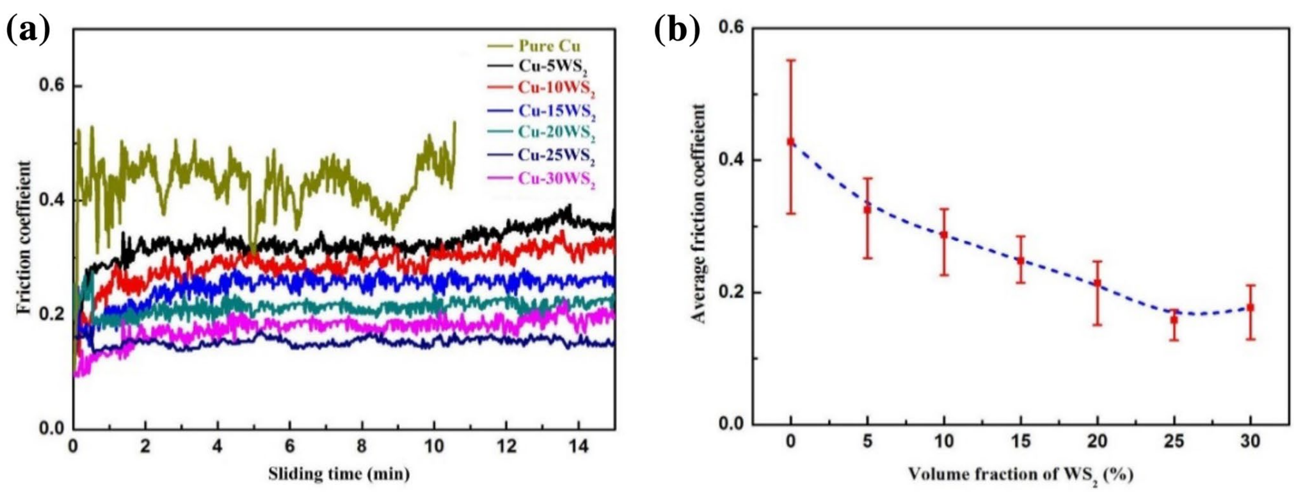

Fig. 5 COF of Cu-WS_2 composites; **a** typical COF curves and **b** average COF values

Cu to 0.21 for the Cu-20WS_2 composite. However, smaller changes were observed when the volume fractions of WS_2 were higher than 20%. The Cu-25WS_2 composite exhibited the lowest COF value of approximately 0.16, which was one-third lower than that of pure Cu. This confirms that adding WS_2 can make a significant difference to the friction, and it can be inferred that the tribo-film which was formed on the sliding surface could provide lubrication (here, it also called a "lubricating film"). Furthermore, the coverage area of the lubricating film that formed during the friction testing was considered to be the reason for the gradual decrease in COF as the solid lubricant content increased [22, 25]. Because of the good shear slip characteristics of the WS_2 particles, the friction process allowed them to continuously rub on the worn surface to form lubricative tribo-films. However, the coverage area of the lubricative tribo-films did not always increase before reaching a predetermined value by adding WS_2, because most of the worn surface was covered with lubricative tribo-films, thus the COF did not change significantly.

The wear track topographies for the Cu-5WS_2 and Cu-25WS_2 composites are shown in Fig. 6a and b, respectively. Generally, the wear volume of the wear track can be calculated based on the wear track depth and the width of the composite after friction testing. As shown in Fig. 6a, the depth and width of the wear tracks of the Cu-5WS_2 composites were approximately 150 and 1800 µm, respectively. In addition, the depth and width of the wear tracks of the Cu-25WS_2 composites decreased to 80 and 1200 µm, respectively. Undoubtedly, the decreased depth and width indicated that adding a certain amount of WS_2 to the Cu matrix could effectively reduce the wear rate.

The average wear rates of the Cu/WS_2 composites according to statistical calculations are shown in Fig. 7. It is obvious that the wear rate of the composites first increased and then decreased as the volume fraction of WS_2 increased. It can be seen from Fig. 7 that the Cu-10WS_2 composites exhibited the highest wear rate. Pure Cu, which exhibits a high COF, presents a fairly low wear rate, which may be caused by its good inner interface bonding ability between the same material phases as well as its high ductility. Materials exhibiting good interface bonding abilities and high ductility can effectively prevent the initiation and propagation of cracks during sliding. It was unexpected that the wear rates of the Cu-5WS_2 and Cu-10WS_2 composites increased considerably as the amount of WS_2 increased. However, as the volume fraction of WS_2 further increased to 25 vol%,

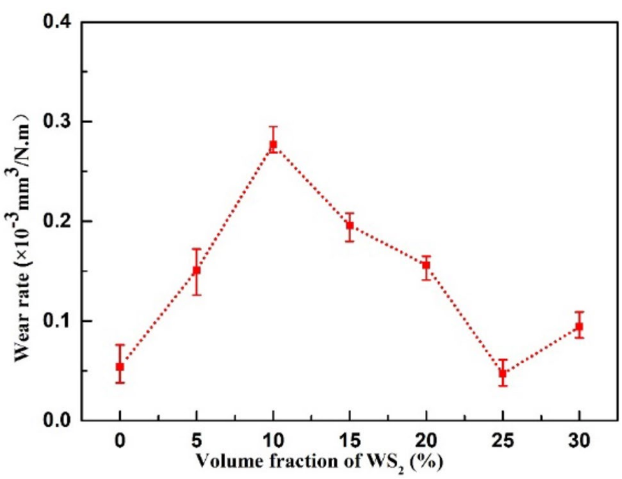

Fig. 7 Variation of average wear rates of Cu/WS_2 composites

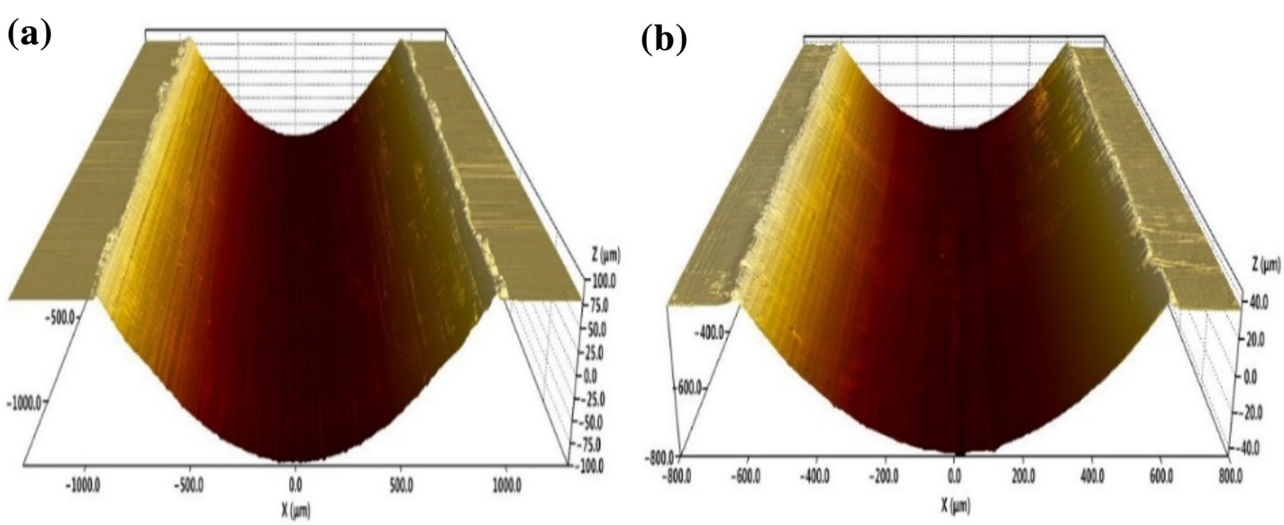

Fig. 6 Wear tracks topography for **a** Cu-5WS_2 and **b** Cu-25WS_2

the wear rates of the composites no longer increased, but decreased dramatically. Similar phenomena have also been observed in other studies [22, 26, 27]. Generally, the COF of the composites is closely related to the tribo-film coverage area on the worn surface and the characteristics of tribo-films. Moreover, the coverage area of the tribo-films largely depends on the amount of solid lubricant WS_2 that was squeezed out from the Cu matrix. More WS_2 squeezed out from the Cu matrix with a higher quantity of added WS_2 in the Cu matrix leads to a higher possibility of the formation of a tribo-film with a full coverage area on the wear track. When the volume fraction of added WS_2 was relatively small (less than 10 vol%), the mechanical properties of the composites was reduced. In this case, the WS_2 squeezed out from the Cu matrix was not enough to form a tribo-film with full coverage area. Thus, the wear rate increased while the COF decreased with the added WS_2. However, when more WS_2(10–25 vol%) was added into the Cu matrix, the WS_2-rich tribo-film forming on the wear track can effectively weaken the contact between the Cu matrix and the counterpart. The shear strength between WS_2 layers was relatively small, so both the wear rate and the COF decreased. When too much WS_2 (more than 25 vol%) was added into the Cu matrix, the disadvantages of the added WS_2 surpassed its advantages in improving tribological properties, leading to an enhanced wear rate. The reason is that too much WS_2 will lead to pores and cracks, which are detrimental to the mechanical properties of the composite [28].

3.3 Worn Surface and Composition Analysis

Figure 8 shows the SEM images of the worn surfaces of the Cu/WS_2 composites. For pure Cu, severe cracks, adhesion spalling pits, and smeared metal layers were observed on the surface, as shown in Fig. 8a. Because of the good plasticity of pure Cu, the strain hardening and fine crystal structure were caused by the friction force. Then, the plastic deformation ability of Cu became poor, leading to fatigue cracks. Moreover, during friction, new worn surfaces and friction-induced heat will be continuously generated. As a result, adhesive wear will most probably occur between the Cu and the counterpart, and oxidation will also take place due to the exposure of the specimen to air atmosphere. Such a phenomenon has also been observed in many other Cu matrix composites [21, 29]. Thus, this indicated that the main wear mechanisms of pure Cu are adhesive and oxidation wear.

The worn surface topographies of the Cu/WS_2 specimens were totally different from that of pure Cu, as shown in Fig. 8b–g. Adhesive pits were rarely observed while smeared metal layers and grooves were seen on the worn surface. The forming of smeared metal layers was closely related to the repetitive grinding process on the wear track and the continuous formation of wear debris. Due to the continuous positive pressure acted on the worn surface, plastic deformation occurred and the fresh wear debris would be rolled repeatedly, leading to the formation of the smeared metal layers. The grooves on the wear track were believed to be generated by the hard asperities on the counterpart and the wear debris plowing and grinding over the softer Cu matrix. Moreover, it can also be inferred from the topography of the worn surfaces that a tribo-film was formed on them. Furthermore, the coverage area of the tribo-film increased gradually and the worn surface became smoother with WS_2 ranging from 5 to 25 vol%. However, the coverage area of the tribo-film as well as the surface roughness decreased when the WS_2 in the specimens exceeded 25 vol%. This may explain why Cu-10WS_2 exhibited the highest wear rate in all the Cu/WS_2 specimens. By comparing the topography of the worn surface to that of pure Cu, as shown in Fig. 8a, it can be concluded that the friction and wear mechanisms are quite different for the former, the tendency of adhesive and oxidation wear was greatly reduced, ande the tendency of delamination and plowing was increased. The higher magnification image of zone A in Fig. 8a is shown in Fig. 8h. Many traces of cracks propagation can be clearly observed which confirmed the formation process of adhesive spalling pits. When the size of cracks increased beyond certain critical dimensions, materials between the surface and the cracks could be removed from the copper matrix and become debris after rubbing between the contact surfaces. Figure 8i, j are enlarged views of the worn surfaces of zones B and C in Fig. 8b, f, respectively. It can be clearly seen that some smeared metal layers bulged on the tribo-film. More cracks can also be observed between the smeared metal layer and the tribo-film on the wear track of the Cu-5WS_2 specimen than that of the Cu-25WS_2 specimen. The phenomenon of was also indirectly related to the COF curve, as shown in Fig. 6a. In summary, adding less than 25 vol% WS_2 to Cu can effectively improve the tribological properties of the material, while adding too much WS_2 was detrimental to the mechanical and tribological properties of the material under the current running conditions.

Figure 9 shows the EDS spectrum analysis of the worn surface of Cu-25WS_2 after sliding wear testing. As shown in Fig. 9a, the surface of the material mainly consisted of a bright phase and a gray phase, where the main elements of the bright phase were W and S, as shown in Fig. 9b, c. It was suggested that the bright phase may contain a large number of WS_2 while the gray phase mainly represents the Cu matrix. However, the distribution of W and S after sliding wear testing was significantly different from that of the surface before testing. This was due to the friction process, when the tribo-film formed and uniformly covered the surface of the material, thereby leading to a good lubrication effect. We further analyzed the bright region in Fig. 9a using EDS, and the results are shown

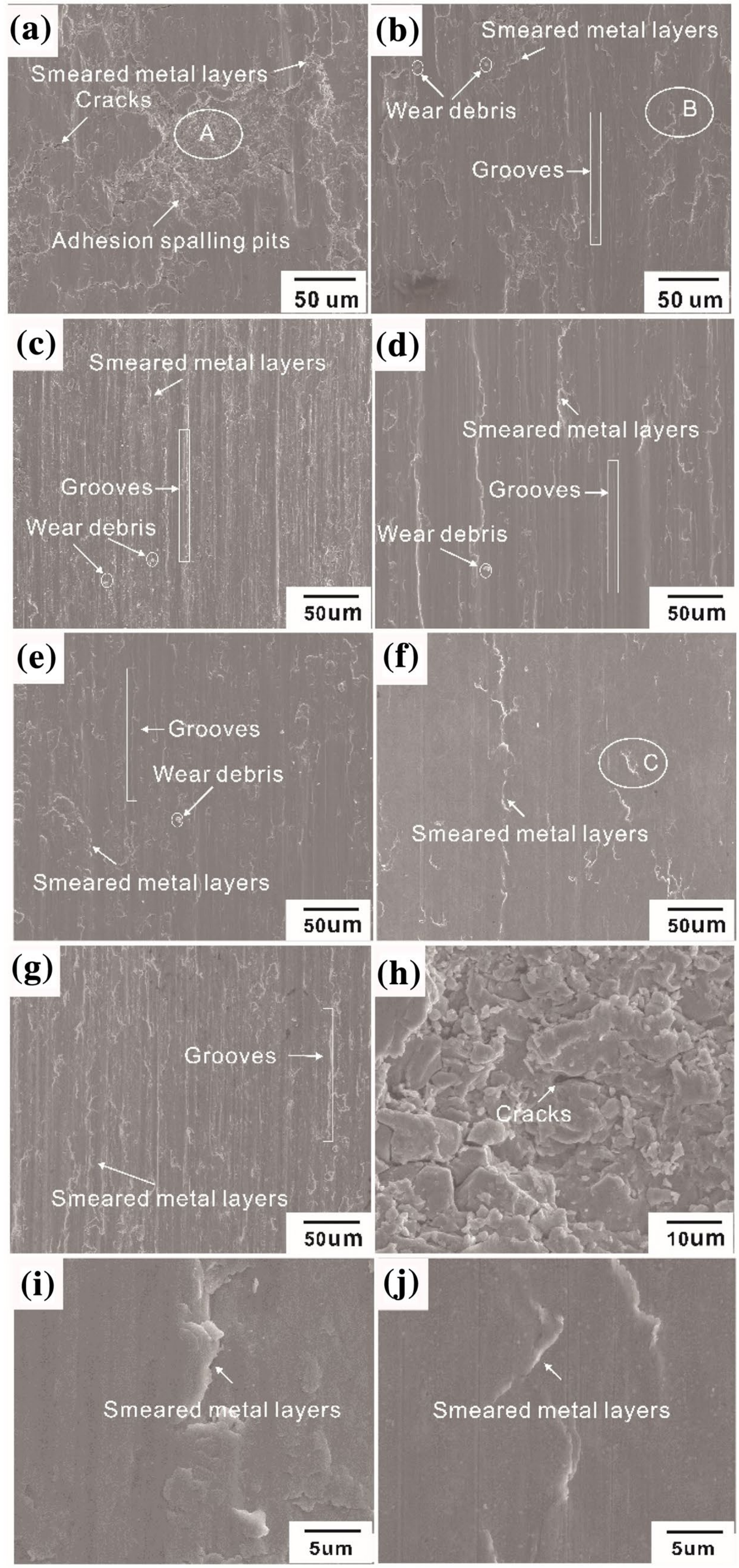

Fig. 8 SEM images of worn surface of Cu/WS_2 composites containing **a** 0, **b** 5, **c** 10, **d** 15, **e** 20, **f** 25, and **g** 30 vol% WS_2; **h**–**j** highly magnified images of zones *A*–*C*, respectively

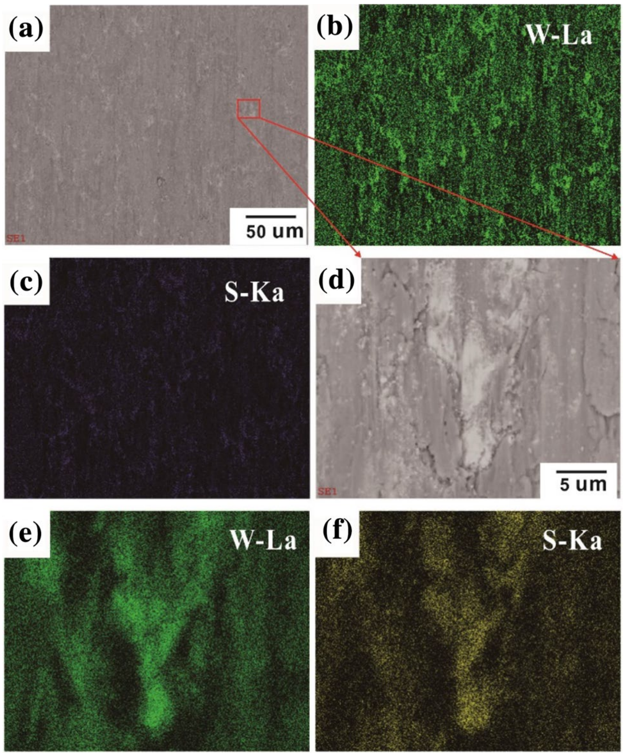

Fig. 9 EDS analysis results on the worn surface of the Cu-25WS_2 composite

in Fig. 9d–f. It was found that the bright phase presented obvious smearing effects on the surface of the wear track. Therefore, it can also be inferred that some bright phase may fill the microcracks or pits on the wear track because of WS_2. Furthermore, according to the EDS analysis, as shown in Fig. 9e, f, it could be concluded that the phase contained a large number of WS_2 and probably a small amount of Cu_2S. Generally, these sulfides benefit the formation of lubricating tribo-films.

The elements from a random area scan on the wear tracks of the Cu/WS_2 specimens were measured by EDS using the same acceleration voltage and acquisition time. The measured weight fractions of W + S in the composites and the calculated weight fractions of W + S which were obtained by calculating the WS_2 addition are shown in Fig. 10. It is easy to see that the measured value of the total W and S was higher than the calculated value, and that there was a prominent bulge on the dotted line marked in the figure as the WS_2 increased from 10 to 25 vol%. This indicated that the friction process might make the WS_2 and the Cu_2S inside the composites become squeezed out and aggregated on the tribo-surface [30]. Therefore, it becomes an important component of the tribo-film. In addition, the phenomenon was obvious when the WS_2 was added to Cu/WS_2 specimens between 10 and 25vol%.

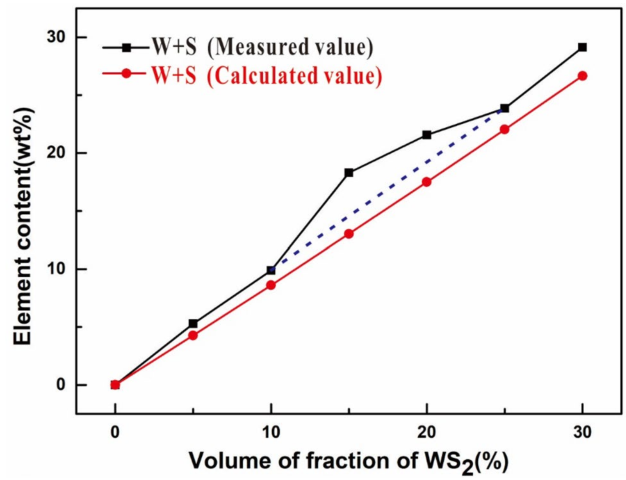

Fig. 10 Measured value and calculated value of W + S on the worn surface for the Cu/WS_2 specimens

3.4 Analysis of Tribo-Film

The above tests and analysis have confirmed that a tribo-film consisting of WS_2 and Cu_2S was present on the worn surface. To investigate the thickness and composition of the tribo-film, the wear track of the Cu-25WS_2 composite was characterized using the XPS etching analysis technique. As seen in Fig. 11a, the intensities of two Cu2p peaks in the XPS spectrum were 932.5 and 952.3 eV, respectively. As the Ar^+ ion etching time increased, both the etching depth and Cu content increased. However, the XPS spectra of S2p and W4f in the depth direction, as shown in Fig. 11b, c, respectively, were obviously different from that of Cu2p. The XPS spectra for S2p and W4f exhibited almost the same tendencies in the depth direction spectrum. Due to the inconsistencies in the change trends, it can be inferred that the components of the tribo-film may not be entirely composed of WS_2, and some Cu_2S could be detected on the worn surfaces. The XPS spectrum of O1s presented an opposite trend compared to that of Cu2p, as shown in Fig. 11d. Before the etching process started, the content of O1s was quite high. This was caused by the surface of the material adsorbing oxygen from the atmosphere through physical or chemical processes. This could have caused the contents of other components to be relatively reduced. Figure 11e shows the depth profile of the worn surface of the Cu-25WS_2 composite. The results showed that, due to the influence of the oxygen adsorption on the surface, the contents of other elements were lower during the early stages of non-etching. After removing the oxygen on the surface by etching, the contents of other elements gradually increased, and the elements found in highest amounts on the surface of the material were S and W. This indicated that the main components of the surface lubricating film were S and W. The amounts

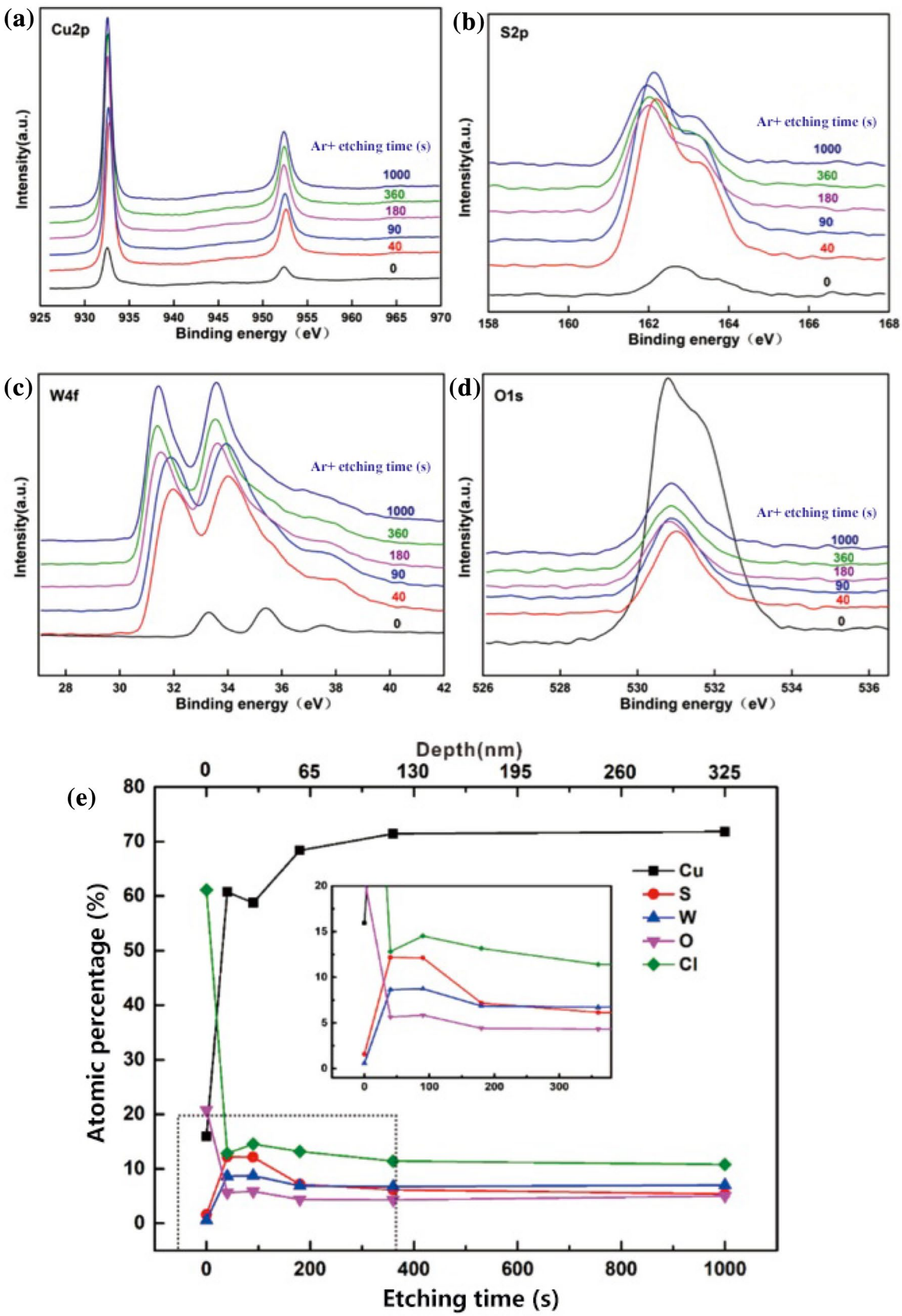

Fig. 11 Evolution of XPS spectra as a function of etching time acquired on the worn surface of the Cu-25 WS_2 composite

of S and W were rapidly reduced after etching the surface for 90 s. Moreover, when the etching time exceeded 180 s, no significant changes were observed in the atomic ratios of S and W on the surface, which indicated that the tribo-film containing higher S and W amounts had been etched away. Moreover, the total amounts of W and S were also equivalent to the content of WS_2 added to the material, and XPS etching had been stopped at the time. Since the XPS etching rate was 0.33 nm/s, we could use the etching time of 180 s to calculate that the maximum thickness of the tribo-film containing WS_2 and Cu_2S was approximately 60 nm.

To further analyze the characteristics, the composition of the tribo-film and the combination between different layers, a TEM sample was cut from the worn surface of the Cu-25WS_2 specimen using FIB, as shown in Fig. 12a. Figure 12b illustrates a snapshot of the final TEM sample from the worn surface and the protective layer of Pt can be clearly observed. From the foregoing analysis, it can be predicted that the tribo-film should be under this protective layer. In addition, Fig. 12c shows the bright field TEM of the highlighted region in Fig. 12b at a higher magnification from which can be seen the tribo-film located between the Pt protective layer and the Cu/WS_2 matrix composites. There were two kinds of morphology of the Pt protective layer because it was coated by an electron beam and an ion beam, respectively. Meanwhile, some small stripes were found in the tribo-film which might be due to a large number of shear and plastic deformations occurring during the friction testing. Also, there might be a good bonding

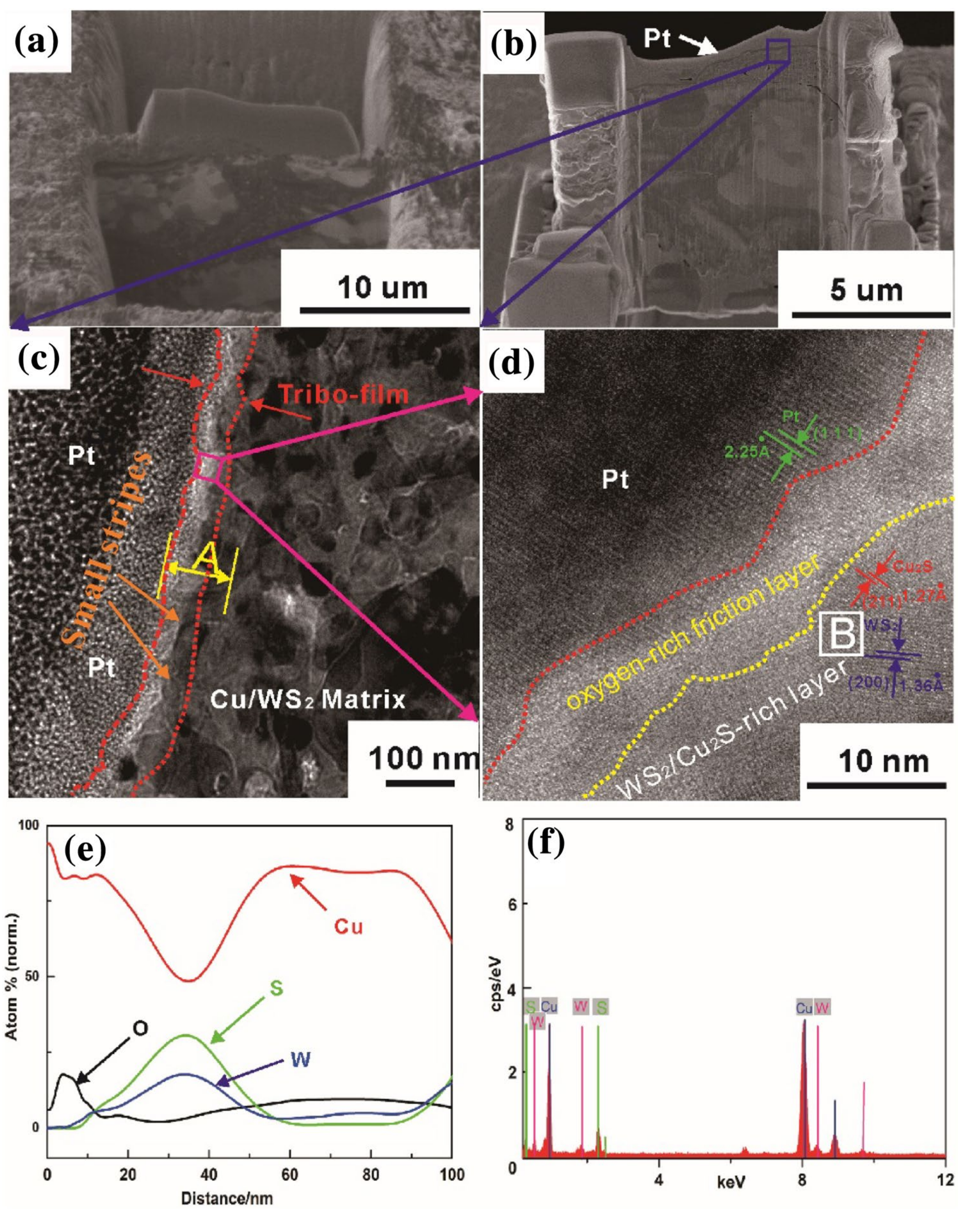

Fig. 12 **a** and **b** SEM images of the TEM sample collected from the worn surface of the Cu-25WS_2 composite, **c** TEM image of the highlighted region in (**b**), **d** HRTEM image of corresponding region in (**c**), **e** EDS line scanning of the region marked *A* in (**c**), **f** EDS area scanning of the region marked *B* in (**d**)

between the tribo-film and the Cu/WS_2 matrix because no obvious cracks were observed at the interface.

To determine the composition and phase distribution of the tribo-film, an HRTEM micrograph of the highlighted region in Fig. 12c is presented in Fig. 12d. The EDS line and area scanning images of the region marked by A in Fig. 12c and the region marked by B are shown in Fig. 12e and f, respectively. Combined with Banalysis resulting from Fig. 12c–f, it can be concluded that there were two different layers in the tribo-film, one with an irregular arrangement of atoms, which is the oxygen-rich friction layer about 10 nm thick, while the other is about 50 nm thick and called WS_2/Cu_2S-rich layer. In addition, the oxygen-rich friction layer was mainly composed of Cu and O while the other layer was rich in W and S. Also, WS_2 and Cu_2S with the crystal indices of (211) and (200) were analyzed by FFT, respectively. Thus, it could be confirmed that the phases in WS_2/Cu_2S-rich layer mainly contained WS_2 and Cu_2S, and provided evidence that the Cu_2S and WS_2 would be squeezed out to form the tribo-film, which could effectively reduce the direct contact between the counterpart and BCu/WS_2 composites. This played an important role in reducing the COF and wear rates [31, 32]. Meanwhile, the irregularly atomic arrangement might due to a large number of shear and plastic deformations occurring during the friction testing. What is more, all the results here were in good agreement with the results of BXPS analysis.

Generally speaking, the way that most self-lubricating composites reduce the COF is due to their low shear strength between layers. However, in this work, the formation of the oxygen-rich layer could potentially increase the shear strength. The reason why there was no increase in the COF and wear rates was closely related to the contact from the point to the surface (ball to block) in the friction testing, and it was quite different from the contact from surface to surface. According to the results previously reported in the literature, Bowden's and Xiao's [33, 34] ball to block tests were caused by the combination of adhesion and plowing. Thus, the tangential force (Ft) and the COF (μ) can then be written as

$$F_t = F_a + F_p \tag{4}$$

$$\mu = \frac{F_a}{F_n} + \frac{F_p}{F_n} = \mu_a + \mu_p \tag{5}$$

where Fa is the adhesion force between the indenter and the contacting material, Pp is the plow force by the plastic deformation material, F_n is the normal force, μ_a is the COF of adhesion, and μ_p is the COF of plowing.

Previous studies [33–38] have shown that the plowing force is generated due to the plastic deformation of the composite while the adhesion force is related to the shearing strength of the interface and contact area. By comparing the only WS_2/Cu_2S-rich layer formed on the worn surface to the WS_2/Cu_2S-rich layer with a thin oxygen-rich friction layer on it, it did not make a great difference to the plastic deformation of the composite. Therefore, the COF of plowing would not obviously change. In addition, the shearing strength of the interface in the oxygen-rich friction layer had increased, but still had a WS_2/Cu_2S-rich layer below it. It is easy to understand that most of the plastic deformation would still occur in the WS_2/Cu_2S-rich layer, because of its lower shear strength. Therefore, it could be concluded that the structure of such a tribo-film would not have a great impact on the shearing strength during friction testing. However, the contact area would be decreased because of the increase in hardness of the tribo-film, so the COF of adhesion decreased and the combination of adhesion and plowing decreased. What is more, the structure of such a tribo-film with higher hardness could effectively isolate the contact between the counterpart and the matrix, which would have a beneficial effect on reducing the wear rate. Thus, it had better wear resistance.

4 Conclusions

Cu/WS_2 composites were prepared by using SPS, and the effect of WS_2 on the microstructures, and tribological properties, especially the tribo-films of the composites, were also investigated. The following conclusions can be drawn:

(1) The COF of the composites decreased significantly when the WS_2 was lower than 20 vol% in the Cu/WS_2 composites, and the COF of the composites did not significantly decrease as the WS_2 increased beyond 20 vol%. The wear rate of the composites first increased and then decreased as the volume fraction of WS_2 increased, and the Cu-10WS_2 composite exhibited the wear rate in this work.
(2) The WS_2 would be squeezed out from the Cu/WS_2 composites to form a tribo-film on the wear track during friction testing, and significant smearing track could be observed on the worn surface.
(3) The tribo-film was approximately 60 nm thick and contained a c.10-nm-thick oxygen-rich friction layer and a c.50-nm-thick WS_2/Cu_2S-rich layer in the Cu-25WS_2 composites.
(4) This structure of the tribo-film could effectively isolate the direct contact between the counterpart and Cu/WS_2 composites, thus reducing the COF and the wear rate. And it may make a guiding role in the design of the tribo-film.

Acknowledgements This work was supported by the National Nature Science Foundation of China. [Grant Number 51475476]. Thanks to Dr. Yang Li, Dr. Xiaoqin Ou and Dr. Hui Deng from Central South University, China for their kind contributions.

References

1. Hammes, G., Schroeder, R., Binder, C., Klein, A.N., deMello, J.D.B.: Effect of double pressing/double sintering on the sliding wear of self-lubricating sintered composites. Tribol. Int. **70**, 119–127 (2014)
2. Lin Liu, Z., Zhang, M., Dienwiebel: The runningin tribological behavior of Pbfree brass and its efect on microstructural evolution. Tribol. Lett. **65**, 160 (2017)
3. Gebretsadik, D.W., Hardell, J., Prakash, B.: Friction and wear characteristics of different Pb-free bearing materials in mixed and boundary lubrication regimes. Wear. 340–341, 63–72 (2015)
4. Moustafa, S.F., El-Badry, S.A., Sanad, A.M., Kieback, B.: Friction and wear of copper-graphite composites made with Cu-coated and uncoated graphite powders. Wear. **253**, 699–710 (2002)
5. Larionova, N.S., Nikonova, R.M., Ladyanov, V.I.: Mechanosynthesis of nanostructured composites copper-fullerite, copper-graphite. Adv. Powder Technol. **29**, 399–406 (2018)
6. Irtegov, Y., An, V., Machekhina, K., Lemachko, N.: Influence of copper nanoparticles on tribological properties of nanolamellar tungsten disulfide. Key Eng. Mater. 133–136 (2016)
7. Jiang, X., Fang, H.C., Xiao, P., Liu, T., Zhu, J.M., Wang, Y.C., Liu, P.F., Li, Y.: Influence of carbon coating with phenolic resin in natural graphite on the microstructures and properties of graphite/copper composites. J. Alloys Compd. **744**, 165–173 (2018)
8. Elkady, O.A.M., Abu-Oqail, A., Ewais, E.M.M., El-Sheikh, M.: Physico-mechanical and tribological properties of Cu/h-BN nanocomposites synthesized by PM route. J. Compd. **625**, 309–317 (2015)
9. Rajkumar, K., Aravindan, S.: Tribological behavior of microwave processed copper–nanographite composites. Tribol. Int. **57**, 282–296 (2013)
10. Zhang, Y., Shockley, J.Michael, Vo, P., Chromik, R.R.: Tribological behavior of cold-sprayed Cu–MoS_2 composite coating during dry sliding wear. Tribol. Lett. **62**, 9 (2016)
11. Kato, H., Takama, M., Iwai, Y., Washida, K., Sasaki, Y.: Wear and mechanical properties of sintered copper-tin composites containing graphite or molybdenum disulfide. Wear. **255**, 573–578 (2003)
12. Linlin Su, F., Gao, X., Han, R., Fu, E., Zhang: Tribological behavior of copper–graphite powder third body on copper-based friction materials. Tribol. Lett. **60**, 30 (2015)
13. Xu, S., Gao, X., Hu, M., Wang, D., Jiang, D. Sun, J., Zhou, F., Weng, L., Liu, W.: Microstructure evolution and enhanced tribological properties of Cu-doped WS_2 films. Tribol. Lett. **55**, 1–13 (2014)
14. An, V., Anisimov, E., Druzyanova, V., Burtsev, N., Shulepov, I., Khaskelberg, M.: Study of tribological behavior of Cu–MoS_2 and Ag–MoS_2 nanocomposite lubricants. SpringerPlus. **5**, 72 (2016)
15. Qian, G., Feng, Y., Li, B., Huang, S., Liu, H., Ding, K.: Effect of electrical current on the tribological behavior of the Cu-WS_2-G composites in air and vacuum. Chin. J. Mech. Eng. **26**, 384–392 (2013)
16. Tyagi, R., Das, A.K., Mandal, A.: Electrical discharge coating using WS_2 and Cu powder mixture for solid lubrication and enhanced tribological performance. Tribol. Int. **120**, 80–92 (2018)
17. Huang, S., Feng, Y., Liu, H., Ding, K., Qian, G.: Electrical sliding friction and wear properties of Cu-MoS_2-graphite-WS_2 nanotubes composites in air and vacuum conditions. Mater. Sci. Eng. A. **560**, 685–692 (2013)
18. Kovalchenko, A.M., Fushchich, O.I., Danyluk, S.: The tribological properties and mechanism of wear of Cu-based sintered powder materials containing molybdenum disulfide and molybdenum diselenite under unlubricated sliding against copper. Wear. 290–291,106–123 (2012)
19. Huiquan, C., Zhiyuan, Q., Lei, Z.: Tribological behavior of Cu matrix composites containing graphite and tungsten disulfide. Tribol. Trans. **6**, 1037–1043 (2014)
20. Wang, Q., Chen, M., Shan, Z., Sui, C., Zhang, L., Zhu, S., Wang, F.: Comparative study of mechanical and wear behavior of Cu/WS_2 composites fabricated by spark plasma sintering and hot pressing. J. Mater. Sci. Technol. **33**, 1416–1423 (2017)
21. Juszczyk, B., Kulasa, J., Malara, S., Czepelak, M., Malec, W., Cwolek, B., Wierzbicki, Ł: Tribological properties of copper-based composites with lubricating phase particles. Arch. Metall. Mater. 59 (2014)
22. Xiao, J., Zhang, W., Liu, L., Zhang, L., Zhang, C.: Tribological behavior of copper-molybdenum disulfide composites. Wear **384–385**, 61–71 (2017)
23. BARIN: Thermochemical Data of Pure Substances, Nai-liang, C.H.E.N.G., et al. transl. Beijing: Science Press. (2003)
24. Liang, Y., Che, Y., Liu, X.: Thermodynamic data manual of inorganic. Northeast University Press, Boston (1993)
25. Su, Y., Zhang, Y., Song, J., Hu, L.: Tribological behavior and lubrication mechanism of self-lubricating ceramic/metal composites: the effect of matrix type on the friction and wear properties. Wear. **372–373**, 130–138 (2017)
26. Lin, C.B., Chang, Z., Tung, Y.H., Ko, Y.: Manufacturing and tribological properties of copper matrix/carbon nanotubes composites. Wear. **270**, 382–394 (2011)
27. Ted Guo, M.L., Tsao, C.Y.A.: Tribological behavior of aluminum/SiC/nickel-coated graphite hybrid composites. Mater. Sci. Eng. A **333**, 134–145 (2002)
28. Chandrakanth, R.G., Rajkumar, K., Aravindan, S.: Fabrication of copper-TiC-graphite hybrid metal matrix composites through microwave processing. Int. J. Adv. Manuf. Technol. **48**, 645–653 (2010)
29. Xiao, Y., Zhang, Z., Yao, P., Fan, K., Zhou, H., Gong, T., Zhao, L., Deng, M.: Mechanical and tribological behaviors of copper metal matrix composites for brake pads used in high-speed trains. Tribol. Int. **119**, 585–592 (2018)
30. Kotnarowski, A.: Selective transfer phenomenon in copper-steel tribological systems. Solid State Phenom. **147–149**, 558–563 (2009)
31. Ejima, T., Saitoh, K., Shinke, N., Taruma, M., Hirai, Y.: Atomic-level analysis of copper sulfide (Cu2S): crystal structure and sliding characteristics. Technology Reports of Kansai University. 54, 23–33(2012)
32. Varenberg, M., Ryk, G., Yakhnis, A., Kligerman, Y., Kondekar, N., McDowell, M.T.: Mechano-chemical surface modification with Cu_2S: inducing superior lubricity. Tribol. Lett. **64**, 28 (2016)
33. Bowden, F.P., Tabor, D.: The friction and lubrication of solids I: Oxford: Clarendon Press (1950)
34. Zhang, J.X.L., Zhou, K.-C., Wang, X.P.: Microscratch behavior of copper–graphite composites. Tribol. Int. **57**, 38–45 (2013)
35. Futami, T., Ohira, M., Muto, H., Sakai, M.: Contact/scratch-induced surface deformation and damage of copper–graphite particulate composites. Carbon. **47**, 2742–2751 (2009)
36. Equey, S., Houriet, A., Mischler, S.: Wear and frictional mechanisms of copper-based bearing alloys. Wear. **273**, 9–16 (2011)
37. Colaco, R., Vilar, R.: A model for the abrasive wear of metallic matrix particle-reinforced materials. Wear **254**, 625–634 (2003)
38. Lafaye, S.: True solution of the ploughing friction coefficient with elastic recovery in the case of a conical tip with a blunted spherical extremity. Wear. **264**, 550–554 (2008)